

Endolithic Microbial Habitats Hosted in Carbonate Nodules Currently Forming within Sediment at a High Methane Flux Site in the Sea of Japan

著者	Yanagawa Katsunori, Shiraishi Fumito, Tanigawa Yusuke, Maeda Toshinari, Mustapha Nurul Asyifah, Owari Satoko, Tomaru Hitoshi, Matsumoto Ryo, Kano Akihiro
journal or publication title	Geosciences
volume	9
number	11
page range	463-1-463-16
year	2019-10-30
その他のタイトル	Endolithic microbial habitats hosted in carbonate nodules currently forming within sediment at a high methane flux site in the sea of Japan
URL	http://hdl.handle.net/10228/00007444

doi: info:doi/10.3390/geosciences9110463

Article

Endolithic Microbial Habitats Hosted in Carbonate Nodules Currently Forming within Sediment at a High Methane Flux Site in the Sea of Japan

Katsunori Yanagawa ^{1,*}, Fumito Shiraishi ², Yusuke Tanigawa ², Toshinari Maeda ³, Nurul Asyifah Mustapha ³, Satoko Owari ⁴ , Hitoshi Tomaru ⁵, Ryo Matsumoto ⁶ and Akihiro Kano ⁷ 

¹ Department of Life and Environment Engineering, Faculty of Environmental Engineering, The University of Kitakyushu, Kitakyushu 808-0135, Japan

² Department of Earth and Planetary Systems Science, Graduate School of Science, Hiroshima University, Higashi-Hiroshima 739-8526, Japan; fshirai@hiroshima-u.ac.jp (F.S.); pcss.tanigawa@gmail.com (Y.T.)

³ Department of Biological Functions Engineering, Graduate School of Life Sciences and Systems Engineering, Kyushu Institute of Technology, Kitakyushu 808-0196, Japan; toshi.maeda@life.kyutech.ac.jp (T.M.); syifah86@yahoo.com (N.A.M.)

⁴ School of Marine Resources and Environment, Tokyo University of Marine Science and Technology, Minato-ku, Tokyo 108-8477, Japan; sowari0@kaiyodai.ac.jp

⁵ Department of Earth Sciences, Graduate School of Science, Chiba University, Chiba 263-8522, Japan; tomaru@chiba-u.jp

⁶ Gas Hydrate Laboratory, Organization for the Strategic Coordination of Research and Intellectual Properties, Meiji University, Chiyoda-ku, Tokyo 101-8301, Japan; ryo_mat@meiji.ac.jp

⁷ Department of Earth and Planetary Science, Graduate School of Science, University of Tokyo, Bunkyo-ku, Tokyo 113-0033, Japan; akano@eps.s.u-tokyo.ac.jp

* Correspondence: kyanagawa@kitakyu-u.ac.jp; Tel.: +81-93-695-3723

Received: 3 October 2019; Accepted: 28 October 2019; Published: 30 October 2019



Abstract: Concretionary carbonates in deep-sea methane seep fields are formed as a result of microbial methane degradation, called anaerobic oxidation of methane (AOM). Recently, active microorganisms, including anaerobic methanotrophic archaea, were discovered from methane seep-associated carbonate outcroppings on the seafloor. However sedimentary buried carbonate nodules are a hitherto unknown microbial habitat. In this study, we investigated the microbial community structures in two carbonate nodules collected from a high methane flux site in a gas hydrate field off the Oki islands in the Sea of Japan. The nodules were formed around sulfate-methane interfaces (SMI) corresponding to 0.7 and 2.2 m below the seafloor. Based on a geochemical analysis, light carbon isotopic values ranging from -54.91‰ to -37.32‰ were found from the nodules collected at the shallow SMI depth, which were attributed to the high contributions of AOM-induced carbonate precipitation. Signatures of methanotrophic archaeal populations within the sedimentary buried nodule were detected based on microbial community composition analyses and quantitative real-time PCR targeted 16S rRNA, and functional genes for AOM. These results suggest that the buried carbonate nodule currently develops AOM-related microbial communities, and grows depending on the continued AOM under high methane flux conditions.

Keywords: carbonate nodule; endolithic microbial community; methane

1. Introduction

A variety of sizes of authigenic carbonates are found in sedimentary environments around deep-sea methane seeps. Among them, loosely-consolidated materials of millimeter- to centimeter-scale

carbonates are called nodules [1–4]. Carbonate nodule formation is caused by elevated supersaturation for carbonate minerals achieved by the shift of chemical equilibrium in dissolved inorganic carbon species. In a methane seep-associated environment, carbonate precipitation is primarily sustained by microbial chemosynthetic reactions, named the anaerobic oxidation of methane coupled with sulfate reduction (AOM) [5]. This microbial reaction produces bicarbonate, increases alkalinity, and eventually causes the precipitation of authigenic carbonates under the anoxic conditions as in the following overall reaction: $\text{CH}_4 + \text{SO}_4^{2-} \rightarrow \text{HCO}_3^- + \text{HS}^- + \text{H}_2\text{O}$ [6,7].

Any microbial strains responsible for AOM have not yet been isolated, despite many intensive studies having been undertaken over many years. Based on culture-independent molecular ecological approaches in various marine settings, including methane seeps, mud volcanoes, and hydrothermal sediments, two primary microbial constituents responsible for the net AOM reaction have been determined over the last two decades, i.e., anaerobic methanotrophic archaea (ANME) and deltaproteobacterial sulfate-reducing bacteria (SRB) or sulfur disproportionating bacteria, which often construct prokaryotic consortia [8–13]. Phylogenetic analyses of the members of the ANME lineages and their syntrophic bacterial partners based on 16S rRNA genes or key functional genes of AOM encoding methyl coenzyme M reductase alpha subunit (*mcrA*) revealed the involvement of several distinct phylogenetic groups, i.e., ANME-1, -2, and -3. The ANME-1 group is divided into two lineages: ANME-1a and -1b [14–16]. They are microscopically detected as single cells, monospecific aggregates, or consortia with SRB [17–19]. The ANME-2 lineages are composed of ANME-2a, -2b, -2c, and -2d subgroups [20–23], all of which are related to culturable Methanosarcinales members. They are known to form aggregates with the SEEP-SRB1 group in *Desulfosarcina/Desulfococcus* [21,24,25] or *Desulfobulbaceae* [26], and non-SRB groups in Betaproteobacteria [26] and Verrucomicrobia [27]. The ANME-3 lineages are often reported from active methane seeps and mud volcanoes. They are related to *Methanococoides* and are found in association with *Desulfobulbaceae* [9].

Several studies on authigenic carbonates in methane-rich seafloor environments have detected microbial biosignatures such as lipid biomarkers [5,28–32], 16S rRNA genes [30,33,34], and carbon isotopic compositions reflective of AOM processes [35,36]. With regards to the organic geochemistry-based study on methane seep carbonate, obtained data, such as biomarker characterization, has mostly been interpreted as a time-integrated sign about historical methanotrophy and past physicochemical conditions related with ancient carbonate precipitation [37]. These pilot studies did not focus on contemporary methanotrophy within the carbonates. In contrast, recent molecular diversity surveys and metabolic activity measurements have demonstrated that the pore spaces in the authigenic seafloor carbonates at methane seep sites were inhabited by active microbial populations including methanotrophic communities [33,38,39]. The active methane consumption by substantial amounts of viable ANME/SRB consortia was sustained in the carbonate matrix at the seafloor in the methane seep site. However, fundamental questions regarding this rocky habitat for microorganisms remain unclear, such as how deep carbonate-hosted microbial communities exist. So far, geomicrobiological analyses of the carbonate-hosted AOM have exclusively focused on surface sedimentary environments at a depth of up to 0.15 m below the seafloor (mbsf). Therefore, carbonate nodules buried deeper than that depth are a hitherto unknown microbial habitat. Given the influence of AOM to carbon and sulfur cycling in sedimentary environments, endolithic AOM-performing communities within the sedimentary buried carbonate nodule and the extent to which the community differs according to magnitude of methane flux should be evaluated. In this study, we examined two methane-related authigenic carbonate nodules, both of which were collected at the AOM zone offshore of Oki islands in the Sea of Japan. Based on an integrated approach, including carbonate mineralogy, pore water geochemistry, microbial cell abundance quantification, and molecular ecological survey targeting 16S rRNA and *mcrA* genes, we demonstrated differences of methanotrophic community distributions and the geochemical composition of the deeply-buried nodules associated with methane seep habitats.

2. Materials and Methods

2.1. Sampling Sites and Sample Collection

After the initial discovery of a massive gas hydrate outcropping on the seafloor in the Umitaka Spur [40,41], the eastern margin of the Sea of Japan has been intensively investigated from the perspectives of geology, geochemistry, geomicrobiology, and as a future energy resource [42–49]. The study site is located southwest of the Oki Trough in the Sea of Japan (Figure 1), and has recently been confirmed as a gas hydrate accumulation area [45]. Carbonate nodule-bearing sediments were retrieved using a piston corer during the UM14-06 expedition with the R/V *Umitaka-maru* in July 2014. The piston cores were located at high methane flux sites PC1406 (36°33.7016 E, 134°08.8291 E) and PC1407 (36°17.1827 N, 134°12.2157 E) at water depths of 1034 and 1349 m, respectively (Figure 1). The centimeter-scale nodules buried in the hemipelagic mud were collected from the split core liner at 2.2 and 0.7 mbsf of PC1406 and PC1407, respectively. Sediments surrounding the nodules were also collected using a sterilized spatula. These were stored at $-80\text{ }^{\circ}\text{C}$ in a deep freezer until further processing. Before the following experiments, the nodule samples were divided into two groups: outside and inside. The inside samples were repeatedly washed with 6N HCl to strip off the peripheral parts to prevent contamination of the outside parts. Thereafter, the innermost section of the nodule was retrieved using a rock chisel and/or razor blade.

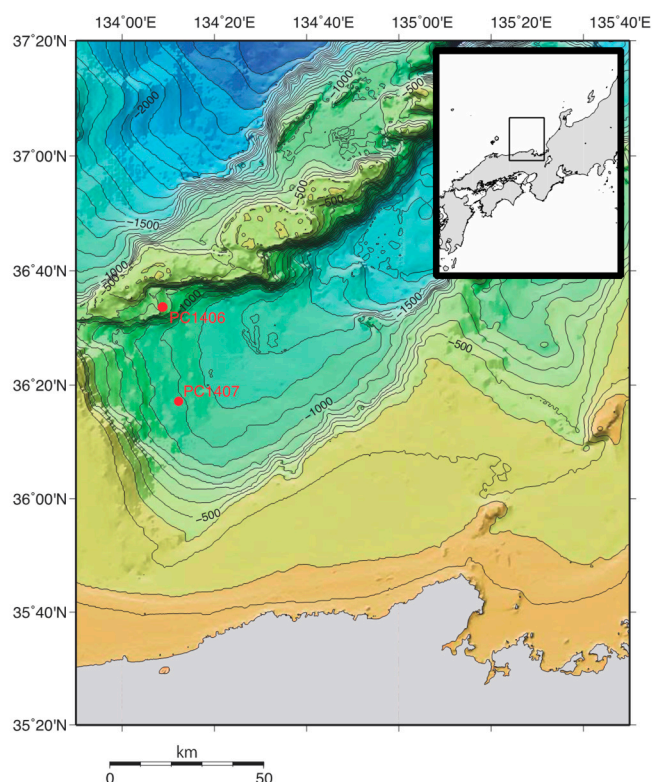


Figure 1. Location of the research area in the eastern margin of the Sea of Japan. Red dots show the location of piston core sampling sites PC1406 and PC1407 during the UM14-06 cruise.

2.2. Pore Water Geochemistry

Pore water was extracted from sediment samples using a hydraulic squeezer with a $0.2\text{ }\mu\text{m}$ disposal disc filter [50]. The concentration of sulfate dissolved in the pore water was measured using an ion chromatograph (ICA-2000, DKK-TOA, Tokyo, Japan) with a PCI230 anion exchange column and electrolytic conductivity detector, as described previously [51]. The concentration of the dissolved methane was determined via the head-space gas method using a gas chromatograph equipped with

a flame ionization detector (GC-4000Plus, GL Sciences, Tokyo, Japan). Total alkalinity (TA) was determined onboard using a spectrophotometer (PD303-S, APEL) [52].

2.3. Mineral and Stable Isotopic Composition of Carbonate Nodules

The mineral composition of the carbonate nodules was examined from a portion of powdered carbonate nodules by X-ray diffraction analysis (XRD; Rint-2100V, Rigaku Corp., Tokyo, Japan). Carbon and oxygen isotopic compositions of the carbonate nodules were measured using a mass spectrometer (Finnigan MAT Delta Plus) accompanied by a Gas Bench [45]. The isotopic values were expressed against VPDB.

2.4. Cell Count

Approximately 0.2 g of the innermost section of the nodule subsamples were fixed with 2% formaldehyde in artificial seawater. After fixation, the samples were washed and replaced with 1 mM EDTA (pH 8.0) to decalcify overnight. The microbial cells collected by centrifuge were concentrated on 0.2 μm pore sized polycarbonate filters (Merck) and enumerated using SYBR Green I, as previously described [53].

2.5. DNA Extraction

Prokaryotic DNA was extracted from approximately 0.2 g of dried and ground nodule subsamples and sediment using the DNeasy PowerSoil Kit (Qiagen) according to the manufacturer's instructions. Microbial cells were mechanically disrupted for 10 min with a $\mu\text{T-01}$ bead crusher (TAITEC, Koshigaya, Japan). The extracted DNA was stored at $-80\text{ }^{\circ}\text{C}$ until the polymerase chain reaction (PCR) analyses.

2.6. Quantitative Real-time PCR (Q-PCR)

Total prokaryotic 16S rRNA gene numbers were determined by Q-PCR using a universal primer-probe set, an archaea-specific primer-probe set [54], and an innuMIX qPCR MasterMix Probe (Analytik Jena AG, Germany). The amplification conditions were 50 cycles of denaturation at $98\text{ }^{\circ}\text{C}$ for 10 s, annealing at $50\text{ }^{\circ}\text{C}$ (universal 16S rRNA gene) or $52\text{ }^{\circ}\text{C}$ (archaeal 16S rRNA gene) for 45 s, and an extension at $72\text{ }^{\circ}\text{C}$ for 30 s. For Q-PCR analyses, the targeted *mcrA* gene, specific primer set [55], and MightyAmp for Real-Time (TaKaRa Bio, Inc., Otsu, Japan) were used under the amplification conditions of 40 cycles of denaturation for 40 s at $94\text{ }^{\circ}\text{C}$, annealing at $52\text{ }^{\circ}\text{C}$ for 30 s, and extension at $68\text{ }^{\circ}\text{C}$ for 60 s. Thermal cycling for Q-PCR was performed with a real-time PCR system qTOWER³ G touch (Analytik Jena AG, Germany). All Q-PCR assays were performed in triplicate. Non-specific amplification of the *mcrA* gene was confirmed by melting curve analysis and gel electrophoresis of the PCR product.

2.7. *McrA* Gene Clone Library Analysis

The *mcrA* gene fragments were amplified by PCR using MightyAmp DNA Polymerase Ver.3 (TaKaRa Bio, Inc., Otsu, Japan) and the specific primers [55]. Amplification was performed using the following procedure: 40 cycles of denaturation at $94\text{ }^{\circ}\text{C}$ for 40 s, annealing at $52\text{ }^{\circ}\text{C}$ for 30 s, and extension at $68\text{ }^{\circ}\text{C}$ for 60 s. After gel purification, the amplified PCR products were inserted into the pMD20-T vector (TaKaRa Bio, Inc., Otsu, Japan) and transformed into *Escherichia coli* DH5 α competent cells (TaKaRa Bio, Inc., Otsu, Japan). The inserted DNA of the positive colony was PCR-amplified with M13M4-M13RV primers and sequenced with the M13RV primer. The obtained *mcrA* gene sequence with more than 95% sequence identity was assigned as the same phylotype. Representative sequences were aligned using the CLUSTALW program, and the ambiguous nucleotide positions were refined manually. Phylogenetic trees were constructed by the neighbor-joining method in the ARB software [56]. Bootstrap analysis was performed with 1000 replicates. The *mcrA* gene sequences obtained in this study were deposited in the DDBJ/EMBL/GenBank databases under accession numbers LC504638–LC504661.

2.8. 16S rRNA Gene Phylotype Composition Analysis

The hypervariable V4 region of the prokaryotic 16S rRNA gene was amplified by PCR using universal primers, 515F/806R [57]. PCR amplification with MightyAmp DNA Polymerase was performed using Biometra TAdvanced 96 SG (Biometra, Göttingen, Germany). The PCR amplification conditions were as follows: initial denaturation at 98 °C for 5 min, 35 cycles of denaturation at 98 °C for 30 s, annealing at 55 °C for 30 s, extension at 68 °C for 30 s, and a final extension at 68 °C for 5 min. PCR amplification of the negative control for DNA extraction was used to check potential experimental contamination. The PCR products were purified and processed using Agencourt AMPure XP beads (Beckman Coulter) and a Nextera XT Index Kit (Illumina), respectively. Sequencing was performed using the Illumina MiSeq platform at the Kyushu Institute of Technology. Phylotype composition analyses, including quality assessment, paired-end joining, quality trimming, chimera detection, OTU clustering (97% cut-off), and phylogenetic analyses, were processed using QIIME2 [58]. Representative sequences were assigned at different taxonomic levels using the SILVA 128 database. Raw sequences are available in the Sequence Read Archive under accession numbers DRA009078.

3. Results and Discussion

3.1. Geochemical Characteristics of the Nodule-Bearing Sediment

Pore water sulfate concentrations decreased to below the limit of detection of 0.1 mM with increased sediment depth, whereas methane concentrations increased with an increasing depth of marine sediment, which went deeper than the sulfate-depleted depth (Figure 2). This vertical profile of geochemistry shows a clear transition zone, which is known as the sulfate-methane interface (SMI) or sulfate methane transition zone (SMTZ) [59]. Based on the linear regression slopes of the sulfate concentrations in this study, the depth of SMI likely appeared at approximately 2.2 mbsf and 0.7 mbsf of PC1406 and 1407, respectively. However, the PC1406 core might fail to retain surface sediment due to degassing during retrieval. Given the seawater sulfate value, extrapolation from the linear regression analysis suggested that the SMI existed at >3 mbsf of PC1406. A previous study proposed that the SMI zone reflects the magnitude of upwelling methane flux from the subsurface [60]. Correspondingly, it seems likely that the PC1407 core is under the control of relatively high methane flux. Total alkalinities at PC1406 and PC1407 were higher than those from non-seep sites in the Sea of Japan [43] (Figure 2), suggesting that carbonate precipitation may occur due to high concentrations of dissolved inorganic carbon provided via an AOM reaction. The existence of a carbonate nodule within the sediment supported this idea. The nodules existed at 2.2 and 0.7 mbsf of PC1406 and PC1407, respectively. The depths of the nodules mostly corresponded to the SMI depth, where the AOM reaction is the most energetically favorable. This indicates that the carbonate nodules are currently forming within the sediments due to an ongoing AOM process around the SMI depth.

Mineralogical analysis using XRD identified that both nodules were high magnesian calcite containing quartz. Quartz accounted for up to 28% and 19% (wt) of the nodules PC1406 and PC1407, respectively. These minerals are known as the basic components of marine carbonates around methane seep environments [32,38]. The chemical composition in the pore water, particularly sulfate and magnesium, is considered to control carbonate mineralogy during precipitation [5]. The carbonate nodules in this study are illustrated by the hypothesis that calcite is created in deeper sediment under low sulfate conditions [61].

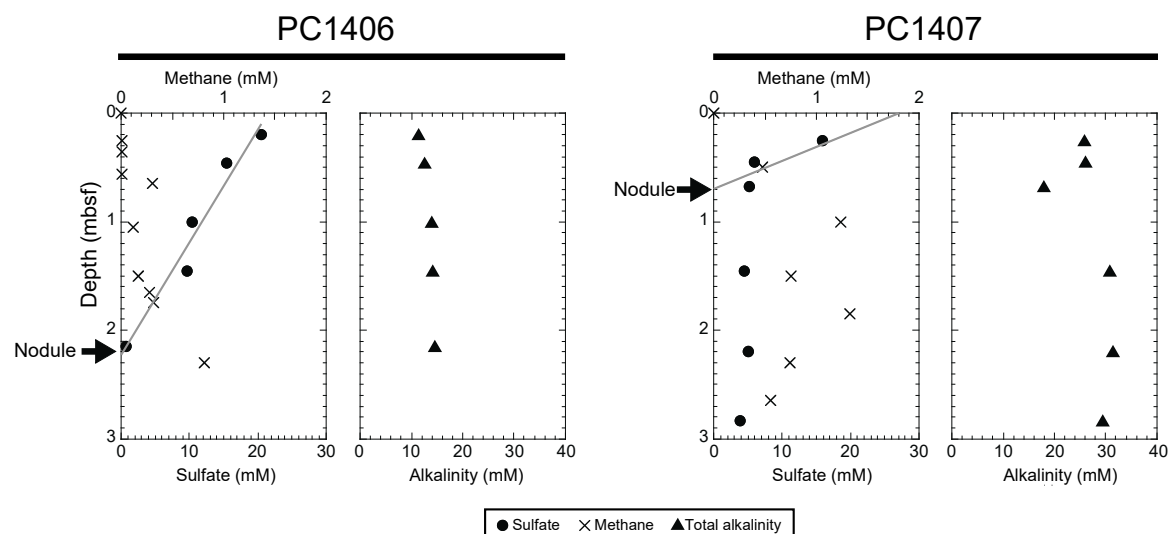


Figure 2. Depth profiles of pore water sulfate, methane, and total alkalinity in the PC1406 and PC1407 cores. Circles, sulfate; crosses, methane; triangles, total alkalinity. Nodules PC1406 and 1407 were collected at the same depth as sulfate-depletion, which was defined by the linear regressions of sulfate.

Carbon isotopic values of the nodules PC 1406 and PC1407 ranged from -38.05‰ to -37.32‰ , and from -54.91‰ to -52.97‰ , respectively (Table 1). There was no statistically significant difference between the inside and outside of the nodules. The more negative carbon isotopic values of the PC1407 nodule indicates that a significant portion of the carbonate carbon originates from methane [61,62]. As the microbial AOM reaction produces ^{13}C -depleted bicarbonate around the SMI depth, the characteristic ^{13}C -depleted carbonate minerals are regarded as products generated by AOM. The nodules were enriched in ^{18}O compared to the expected values for calcite precipitation from pore water in the study site [45]. This is possibly due to the decomposition of gas hydrates.

Table 1. Carbon and oxygen isotopic compositions and microbial cell abundance of carbonate nodules collected from piston cores.

Core	Depth (mbsf)	Sample	$\delta^{13}\text{C}$ (‰)	$\delta^{18}\text{O}$ (‰)	Cell Count (cells/g)
PC1406	2.2	Nodule outside	-37.32	$+4.56$	$1.75 \times 10^7 (\pm 0.37 \times 10^7)$
		Nodule inside	-38.05	$+4.50$	$0.99 \times 10^7 (\pm 0.23 \times 10^7)$
		Sediment	—	—	$2.30 \times 10^7 (\pm 0.11 \times 10^7)$
PC1407	0.7	Nodule outside	-54.91	$+5.12$	$1.45 \times 10^7 (\pm 0.33 \times 10^7)$
		Nodule inside	-52.97	$+5.31$	$0.85 \times 10^7 (\pm 0.14 \times 10^7)$
		Sediment	—	—	$1.08 \times 10^7 (\pm 0.23 \times 10^7)$

These geochemical differences relating to the mineralogy and pore water chemistry were useful for understanding the physical and chemical conditions at the study site during precipitation. It seems likely that high methane flux, expected from shallow SMI depths, increases the AOM rate, and precedes nodule formation within the sediment. Therefore, the buried nodules are probably composed of carbonate derived from ongoing AOM.

3.2. Microbial Abundance in the Nodule

Microscopic observations showed that microbial abundance ranged from 0.85×10^7 to 1.75×10^7 cells per g of the inside and outside of the nodule (Table 1). Most cells were not observed as cell aggregates, but instead as single cells. The cell numbers in the nodule were comparable to those in the adjacent sediment collected at the same depth. Similar microbial abundances were also confirmed by Q-PCR analysis targeting prokaryotic 16S rRNA genes (Figure 3). The whole prokaryotic 16S rRNA

gene numbers ranged from 1.1×10^7 to 8.6×10^7 genes per g of the sample (nodule or sediment). Archaeal 16S rRNA gene abundances were one to two orders of magnitude lower than those of the prokaryotes in the nodule samples, and ranged from 4.3×10^5 to 2.6×10^7 genes per g of the sample.

The abundances of *mcrA*, which are key functional genes for methane-metabolizing archaea [14–20], were also examined using Q-PCR. They were detected only from the nodule PC1407, and were an order of magnitude lower than the archaeal 16S rRNA genes (Figure 3). The *mcrA* gene numbers in the nodule PC1406 were below the limit of detection of 5.0×10^4 genes per g of the sample. The *mcrA* gene abundance in the nodule PC1407 was the same in the adjacent sediment sample collected at the same depth. These results imply that the occurrence of ANME in the nodule is affected by environmental parameters, as represented by the physical and chemical characteristics of the nodule and the surrounding conditions, such as SMI depth.

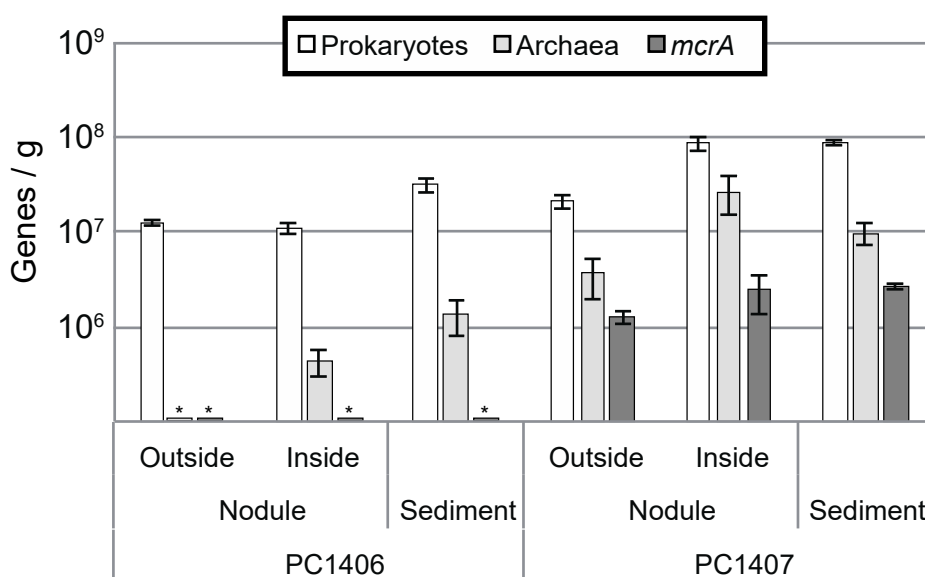


Figure 3. Numbers of 16S rRNA and *mcrA* genes in the nodule and adjacent sediment samples quantified by Q-PCR. An asterisk indicates below the limit of detection.

3.3. *McrA* Phylotype Composition in the Nodule Habitat

Phylogenetic diversity of the *mcrA* gene was determined based on the sequence of the obtained *mcrA* clones (Figure 4). The phylogenetic positions of the *mcrA* genes are divided into several groups, a, b, c, d, e, and f, all of which are distinct from known methanogens. Our results show that the most frequently-obtained sequence in both sediment and nodules at sites PC1406 and PC1407 was related to *mcrA* groups a–b (Figure 4). The a–b groups detected in this study constituted at least 75% of the *mcrA* gene amplicons from the nodule and sediment samples. The *mcrA* a–b groups are possibly hosted by ANME-1 lineages [63]. The *mcrA* gene sequences of groups c–d and e were found as a minority. Because the groups c–d and group e are phylogenetically-congruent with ANME-2c and ANME-2a, respectively [63], ANME-2 archaea were not the dominant archaeal methanotrophs in the study site.

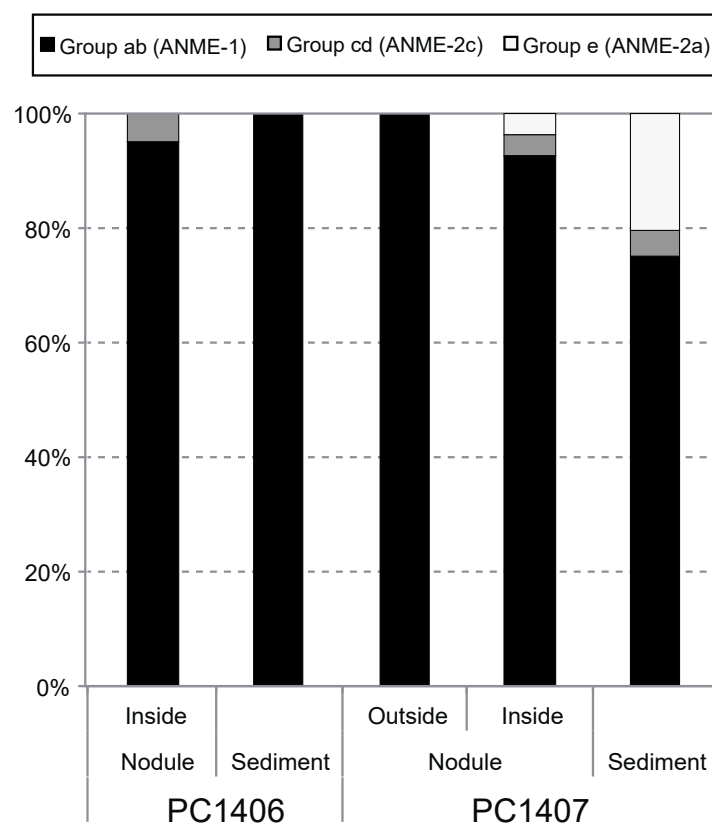


Figure 4. Phylogenetic compositions of *mcrA* genes detected at PC1406 and PC1407 samples.

3.4. Nodule-Hosted Microbial Community Compositions

Prokaryotic community compositions in the nodules and sediment samples were analyzed for comparison between the two coring sites, i.e., PC1406 and PC1407 (Figure 5). All the samples, including the nodules and the surrounding sediments, shared many common phlotypes. The dominant phlotypes in the nodules and sediments were composed of uncultivated archaeal and bacterial members common to typical subsurface environments. The most abundant phlotypes found in our samples were affiliated with phylum Atribacteria, which comprised approximately one-third of the 16S rRNA gene amplicons. Bacterial sequences belonging to the phylum Chloroflexi and class Deltaproteobacteria were also predominantly detected in the nodule and sediment samples. They are known as endolithic microbial members in surface carbonates [38]. Although aerobic methane oxidation has been suggested in cold seep-associated carbonates and sediments [33], 16S rRNA gene sequences belonging to known aerobic methanotrophic bacteria were absent from both nodules and sediment. The most dominant archaeal populations included Lokiarchaeota members of the Asgard superphylum, comprising low percentages of the total gene amplicons in the PC1406 (~12.4%) and PC1407 (~8.2%) nodules (Figure 5). Their physiological characteristics are not well understood. However, they have been substantially detected in many deep-sea sediments associated with high methane flux. In some previous studies, they represent more than half of the phlotype compositions [47,64]. Class Thermoplasmata and Halobacteria were also detected in the archaeal sequences, which belong to the Marine Benthic Group D (also known as the Deep-Sea Hydrothermal Vent Euryarchaeota Group-1) and Woesearchaeota. Most of them appeared to have nothing to do with AOM, suggesting that the microbes endogenously living in sediment were packed into the carbonate nodule by AOM.

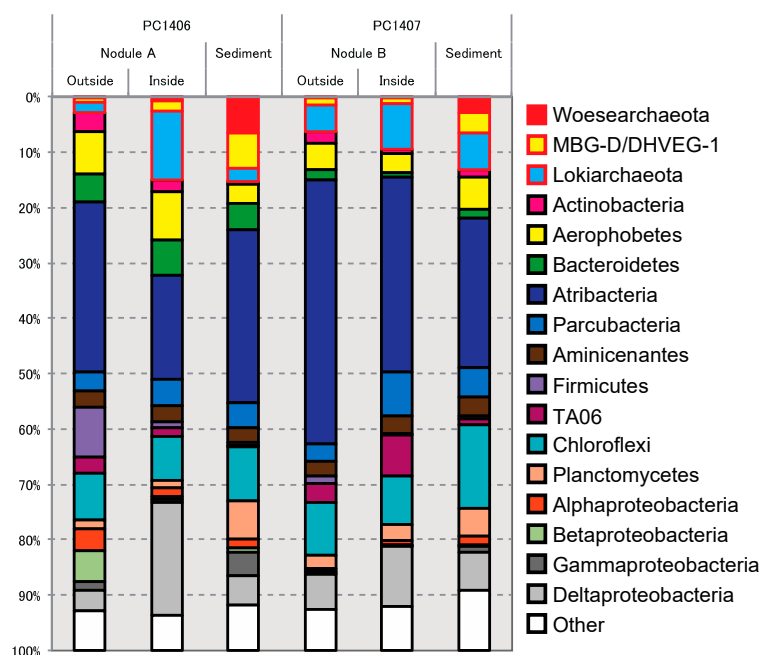


Figure 5. Phylum/class-level phylogenetic affiliations of prokaryotic 16S rRNA gene sequences amplified from the nodule and adjacent sediment samples.

The relative taxa abundances of ANME lineages showed that the ANME-1b group was more predominant than ANME-2 in the nodule and sediment samples (Figure 6). This result was consistent with the *mcrA* gene clone library analysis, as mentioned above. The members of ANME-1b were predominantly comprised of up to approximately 2.4% of the 16S rRNA gene phylotype compositions from the nodule PC1407, whereas the proportions of the ANME-1b populations in the nodule PC1406 ranged between 0.053–0.243% of total gene amplicons. These results are in agreement with previous studies that demonstrated the ANME-1b dominance in the methane-rich sediment in the Sea of Japan [48].

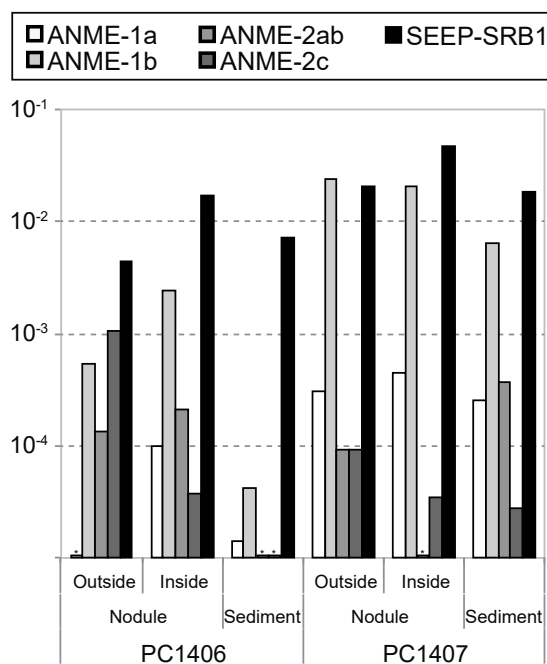


Figure 6. The relative taxa abundance of ANME-1a, -1b, -2ab, -2c, and SEEP-SRB1 members.

ANME archaea have been reported to be associated with a syntrophic sulfate reducer belonging to Deltaproteobacteria to accomplish methane oxidation under anaerobic conditions. In this study, members of SEEP-SRB1 in the Desulfosarcina/Desulfococcus group cooccurred with ANME, accounting for ~4.64% of whole 16S rRNA gene amplicons in the nodule PC1407 (Figure 6). SEEP-SRB1 are putatively syntrophic sulfate reducers and are commonly observed with ANME-1 and -2 in a variety of high methane flux settings [8]. The relative abundances of ANME and SEEP-SRB1 were higher at the PC1407 site than the PC1406 site. One plausible explanation for the presence of ANME/SEEP-SRB1 in the carbonate nodule is the preservation of relic DNA from the AOM consortia in the surrounding sediment. In particular, the carbonate precipitation via the AOM reaction would affect the microbially-habitable pore spaces, possibly accelerating the consolidation of the nodule, and resulting in self-burial of the sediment-host microbial populations into the carbonate nodules [33,38]. Therefore, microbial biomarkers, such as lipids, within the carbonates could be regarded as a proxy of the microbes in the AOM-occurring sediment [29,30,32]. If the carbonate nodule was a passive repository of the preserved ancient microbial DNA, a marked difference in the microbial community would be expected between the carbonate nodule and the adjacent sediments. Our data suggest that similar microbial communities were present in both carbonate and sediment samples. The pore water conditions and isotope geochemistry also provided the feasibility of AOM in the nodule-surrounding environment. Therefore, it is more likely that the methanotrophic community is continually viable and active in the nodule, and that the growth of the nodule is an ongoing process. Further experiments such as RNA analyses, fluorescence in situ hybridization, and activity measurement of AOM will provide conclusive evidence that the AOM communities within the nodule are fueled by methane provided from gas hydrate.

The microbial abundances did not differ significantly between the two nodules; they may have the same habitat capacity for endolithic microorganisms. Porosity and permeability of the nodules are considered important factors for controlling and limiting the habitable zone of the seafloor microbial components [33,65,66]. Regarding the ecological advantage of the habitable zone within the carbonate nodule, it is hypothesized that the carbonate nodule habitat works as a physical buffer against fluctuating chemical conditions in the methane seep environment [39], which could concentrate microbial requirements within the nodule. In contrast, low permeability, indicating the lack of pore connectivity, would limit the transport of chemical substrates, and spatially isolate microbial cells within the nodule interior [67,68]. All these physical constraints may influence microbial growth, abundance, community diversity, and methanotrophic activity.

3.5. AOM-Responsible Microbial Life within the Nodules at the High Methane Flux Site

This study focused on the microbial populations in deeply-buried carbonate nodules at an active methane seep site. The nodule-hosted microbial life is sustained in the restricted habitat due to a plentiful supply of methane. Activities of methane seepage have been visually identified by the growth of methane seep-associated faunal and microbial communities at the seafloor. Chemosynthetic vesicomyid bivalves (genus *Calyptogena*), mussels (genus *Bathymodiolus*), tube worms (family Siboglinidae), and polychaetes often create their faunal colonies around methane seepage [64,69,70]. White mats of sulfur-oxidizing bacteria (*Beggiatoa* or *Thioploca*) are also common around methane seeps. These apparent signatures for methane seepage activity could inspire the temporal change of methane flux from the subsurface. They are effective only if changes in physical and chemical conditions reach the surface sediment.

On the other hand, the seep site with weak methane flux requires other indicators. In this study, to understand the importance of AOM processes on carbonate nodule formation under different methane flux conditions, the pore water sulfate profile in marine sediment was used as a diagnostic indicator of the in situ methane flux. The SMI depth is considered a proxy of in situ methane flux at unapparent methane seep sites [60].

From a broad perspective, microbial populations in methane-rich sediments around gas hydrate sites are distinct from those from the non-active reference sites [34,38,47,71,72]. As the previous studies focusing on surface carbonates reported [33,38,39], our results show the conspicuous distribution of ANME-1b and SEEP-SRB1 populations even in the inside nodule collected at the gas hydrate-bearing sediment. This result suggests that active methane transport from the subsurface may support ANME archaea and play an important role in authigenic carbonate precipitation. Prokaryotic abundance associated with AOM in PC1407 was higher than in PC1406. This is consistent with a previous study on the 16S rRNA gene sequence-based microbial community analyses, which found that ANME populations were highly influenced by methane seep activity [29], methane concentration [73,74], and SMI depth [48]. It has been hypothesized that the ANME subgroup has a preferred habitat related to physicochemical parameters, such as temperature, oxidation reduction potential, concentration of methane, sulfate, sulfide, and oxygen. Specifically, members of the ANME-1 subgroup are often found at deep, reductive, and sulfate-depleted habitats [29,34,48,64,75–79]. Incubation-based experiments showed that ANME-1 seemed to flourish under higher methane partial pressures without regard for sulfate concentration [74].

Furthermore, ANME lineage compositions were likely different based on the magnitude of seep flux [33,39]. These imply that the habitability of ANME-1 in the nodule is controlled by the specific geochemical conditions associated with methane flux. Therefore, it is considered that the microbial signature within the sedimentary buried carbonate nodule was derived not from the ancient or time-integrated signal of the nodule-forming microorganisms, but from the active microbial populations currently living in the nodule.

Members of the ANME archaea contribute to global climate regulation because methane is a significant greenhouse gas. AOM activity is the dominant sink for methane in the marine environment, which eliminates 70–90% of methane released from the underlying subsurface [59,80,81]. In this study, methanotrophic archaeal genes from the sedimentary-buried carbonate nodule may extend the known ecological niche of the AOM communities. The findings in this study indicate that the active methane supply associated with gas hydrate is important for supporting endolithic AOM communities. The geomicrobiological study of marine AOM has historically been conducted at sediment-based habitats. However, methane seep areas are only partially covered with sediment. Methane-derived authigenic carbonate rock is considered to pave methane seeps accounting for a large portion of the area, although accurate information on the global distribution is limited [82]. It is considered that the sedimentary-buried carbonate rock represents a previously-unexplored carbon sink for methane migrated from the subsurface or provided from the shallow gas hydrate. Endolithic AOM would mitigate the methane flux from the ocean to the atmosphere, and has a significant impact on global methane budgets.

4. Conclusions

This study reports the quantitative and qualitative microbial community compositions in the sedimentary buried nodule associated with the gas hydrate at the subseafloor of the Oki Trough in the Sea of Japan. AOM-related microbial populations, such as ANME-1b and SEEP-SRB1, were pervasive, even in the nodule growing below the seafloor at the high methane flux area. The incidence of these microbial populations is most likely controlled by the supply of AOM substrate into the inside of the nodule. The distribution of the methane-consuming community within the nodule interior probably represents the uncharacterized methane sink that should be taken into consideration for global budgets of methane.

Author Contributions: Conceptualization, K.Y.; methodology, K.Y., F.S., Y.T., T.M., N.A.M., S.O., and A.K.; data Curation, K.Y., F.S., Y.T., T.M., N.A.M., S.O., and H.T.; writing – original draft preparation, K.Y.; writing – review & editing, K.Y.; project administration, K.Y., R.M., and A.K.; funding acquisition, K.Y., F.S., T.M., R.M., and A.K.

Funding: This research was funded by the Challenging Research (17K18808, to K.Y.), Grant-in-Aid for Young Scientists (15H05335, to K.Y.), and Grants-in-Aid for Scientific Research (25800280 and 16H06022, to F.S.) from the Japan Society for the Promotion of Science (JSPS).

Acknowledgments: We thank the shipboard science party of the UM14-06 cruise and the captain and crews of the R/V *Umitaka-maru* for their help in sample collection.

Conflicts of Interest: The authors declare no conflict of interest.

References

1. Orphan, V.J.; Ussler, W.; Naehr, T.H.; House, C.H.; Hinrichs, K.U.; Paull, C.K. Geological, geochemical, and microbiological heterogeneity of the seafloor around methane vents in the Eel River Basin, offshore California. *Chem. Geol.* **2004**, *205*, 265–289. [[CrossRef](#)]
2. Watanabe, Y.; Nakai, S.; Hiruta, A.; Matsumoto, R.; Yoshida, K. U-Th dating of carbonate nodules from methane seeps off Joetsu, Eastern Margin of Japan Sea. *Earth. Planet. Sci. Lett.* **2008**, *272*, 89–96. [[CrossRef](#)]
3. Hiruta, A.; Klügel, A.; Matsumoto, R. Increase in methane flux and dissociation of iron and manganese oxides recorded in a methane-derived carbonate nodule in the eastern margin of the Sea of Japan. *GeoRes* **2016**, *9*, 104–116. [[CrossRef](#)]
4. Mason, O.U.; Case, D.H.; Naehr, T.H.; Lee, R.W.; Thomas, R.B.; Bailey, J.V.; Orphan, V.J. Comparison of archaeal and bacterial diversity in methane seep carbonate nodules and host sediments, Eel River Basin and Hydrate Ridge, USA. *Microb. Ecol.* **2015**, *70*, 766–784. [[CrossRef](#)] [[PubMed](#)]
5. Aloisi, G.; Bouloubassi, I.; Heijs, S.K.; Pancost, R.D.; Pierre, C.; Sinninghe Damsté, J.S.; Gottschal, J.C.; Forney, L.J.; Rouchy, J.-M. CH₄-consuming microorganisms and the formation of carbonate crusts at cold seeps. *Earth Planet. Sci. Lett.* **2002**, *203*, 195–203. [[CrossRef](#)]
6. Valentine, D.L. Biogeochemistry and microbial ecology of methane oxidation in anoxic environments: A review. *Anton. Leeuw. Int. J. G.* **2002**, *81*, 271–282. [[CrossRef](#)]
7. Valentine, D.L.; Reeburgh, W.S. New perspectives on anaerobic methane oxidation. *Environ. Microbiol.* **2000**, *2*, 477–484. [[CrossRef](#)]
8. Knittel, K.; Boetius, A. Anaerobic oxidation of methane: Progress with an unknown process. *Annu. Rev. Microbiol.* **2009**, *63*, 311–334. [[CrossRef](#)]
9. Lösekann, T.; Knittel, K.; Nadalig, T.; Fuchs, B.; Niemann, H.; Boetius, A.; Amann, R. Diversity and abundance of aerobic and anaerobic methane oxidizers at the Haakon Mosby mud volcano, Barents Sea. *Appl. Environ. Microbiol.* **2007**, *73*, 3348–3362. [[CrossRef](#)]
10. Scheller, S.; Yu, H.; Chadwick, G.L.; McGlynn, S.E.; Orphan, V.J. Artificial electron acceptors decouple archaeal methane oxidation from sulfate reduction. *Science* **2016**, *351*, 703–707. [[CrossRef](#)]
11. Milucka, J.; Ferdelman, T.G.; Polerecky, L.; Franzke, D.; Wegener, G.; Schmid, M.; Lieberwirth, I.; Wagner, M.; Widdel, F.; Kuypers, M.M.M. Zero-valent sulphur is a key intermediate in marine methane oxidation. *Nature* **2012**, *491*, 541. [[CrossRef](#)] [[PubMed](#)]
12. McGlynn, S.E.; Chadwick, G.L.; Kempes, C.P.; Orphan, V.J. Single cell activity reveals direct electron transfer in methanotrophic consortia. *Nature* **2015**, *526*, 531. [[CrossRef](#)] [[PubMed](#)]
13. Wegener, G.; Krukenberg, V.; Riedel, D.; Tegetmeyer, H.E.; Boetius, A. Intercellular wiring enables electron transfer between methanotrophic archaea and bacteria. *Nature* **2015**, *526*, 587. [[CrossRef](#)] [[PubMed](#)]
14. Hallam, S.J.; Putnam, N.; Preston, C.M.; Detter, J.C.; Rokhsar, D.; Richardson, P.M.; DeLong, E.F. Reverse methanogenesis: Testing the hypothesis with environmental genomics. *Science* **2004**, *305*, 1457–1462. [[CrossRef](#)] [[PubMed](#)]
15. Hinrichs, K.U.; Hayes, J.M.; Sylva, S.P.; Brewer, P.G.; DeLong, E.F. Methane-consuming archaeobacteria in marine sediments. *Nature* **1999**, *398*, 802–805. [[CrossRef](#)]
16. Meyerdierks, A.; Kube, M.; Lombardot, T.; Knittel, K.; Bauer, M.; Glockner, F.O.; Reinhardt, R.; Amann, R. Insights into the genomes of archaea mediating the anaerobic oxidation of methane. *Environ. Microbiol.* **2005**, *7*, 1937–1951. [[CrossRef](#)] [[PubMed](#)]
17. Orphan, V.J.; House, C.H.; Hinrichs, K.U.; McKeegan, K.D.; DeLong, E.F. Multiple archaeal groups mediate methane oxidation in anoxic cold seep sediments. *Proc. Natl. Acad. Sci. USA* **2002**, *99*, 7663–7668. [[CrossRef](#)]
18. Treude, T.; Krüger, M.; Boetius, A.; Jørgensen, B.B. Environmental control on anaerobic oxidation of methane in the gassy sediments of Eckernförde Bay (German Baltic). *Limnol. Oceanogr.* **2005**, *50*, 1771–1786. [[CrossRef](#)]

19. Yanagawa, K.; Tomaru, H.; Sunamura, M.; Matsumoto, R. Thermodynamic control on anaerobic oxidation of methane below the sulphate-methane interface. In Proceedings of the 7th International Conference on Gas Hydrates, Scotland, UK, 17–21 July 2011.
20. Orphan, V.J.; House, C.H.; Hinrichs, K.U.; McKeegan, K.D.; DeLong, E.F. Methane-consuming archaea revealed by directly coupled isotopic and phylogenetic analysis. *Science* **2001**, *293*, 484–487. [[CrossRef](#)]
21. Yanagawa, K.; Morono, Y.; Beer, D.d.; Haeckel, M.; Sunamura, M.; Futagami, T.; Hoshino, T.; Terada, T.; Nakamura, K.-L.; Urabe, T.; et al. Metabolically active microbial communities in marine sediment under high-CO₂ and low-pH extremes. *ISME J.* **2013**, *7*, 555–567. [[CrossRef](#)]
22. Haroon, M.F.; Hu, S.; Shi, Y.; Imelfort, M.; Keller, J.; Hugenholtz, P.; Yuan, Z.; Tyson, G.W. Anaerobic oxidation of methane coupled to nitrate reduction in a novel archaeal lineage. *Nature* **2013**, *500*, 567. [[CrossRef](#)] [[PubMed](#)]
23. Ino, K.; HERNSDORF, A.W.; KONNO, U.; Kouduka, M.; Yanagawa, K.; Kato, S.; Sunamura, M.; Hirota, A.; Togo, Y.S.; Ito, K.; et al. Ecological and genomic profiling of anaerobic methane-oxidizing archaea in a deep granitic environment. *ISME J.* **2018**, *12*, 31–47. [[CrossRef](#)] [[PubMed](#)]
24. Boetius, A.; Ravensschlag, K.; Schubert, C.J.; Rickert, D.; Widdel, F.; Gieseke, A.; Amann, R.; Jørgensen, B.B.; Witte, U.; Pfannkuche, O. A marine microbial consortium apparently mediating anaerobic oxidation of methane. *Nature* **2000**, *407*, 623–626. [[CrossRef](#)]
25. Kleindienst, S.; Ramette, A.; Amann, R.; Knittel, K. Distribution and in situ abundance of sulfate-reducing bacteria in diverse marine hydrocarbon seep sediments. *Environ. Microbiol.* **2012**, *14*, 2689–2710. [[CrossRef](#)] [[PubMed](#)]
26. Pernthaler, A.; Dekas, A.E.; Brown, C.T.; Goffredi, S.K.; Embaye, T.; Orphan, V.J. Diverse syntrophic partnerships from deep-sea methane vents revealed by direct cell capture and metagenomics. *Proc. Natl. Acad. Sci. USA* **2008**, *105*, 7052–7057. [[CrossRef](#)] [[PubMed](#)]
27. Hatzenpichler, R.; Connon, S.A.; Goudeau, D.; Malmstrom, R.R.; Woyke, T.; Orphan, V.J. Visualizing in situ translational activity for identifying and sorting slow-growing archaeal–bacterial consortia. *Proc. Natl. Acad. Sci. USA* **2016**, *113*, E4069–E4078. [[CrossRef](#)]
28. Peckmann, J.; Thiel, V. Carbon cycling at ancient methane–seeps. *Chem. Geol.* **2004**, *205*, 443–467. [[CrossRef](#)]
29. Blumenberg, M.; Seifert, R.; Reitner, J.; Pape, T.; Michaelis, W. Membrane lipid patterns typify distinct anaerobic methanotrophic consortia. *Proc. Natl. Acad. Sci. USA* **2004**, *101*, 11111–11116. [[CrossRef](#)]
30. Stadnitskaia, A.; Nadezhkin, D.; Abbas, B.; Blinova, V.; Ivanov, M.K.; Damste, J.S.S. Carbonate formation by anaerobic oxidation of methane: Evidence from lipid biomarker and fossil 16S rDNA. *Geochimi. Cosmochimi. Acta* **2008**, *72*, 1824–1836. [[CrossRef](#)]
31. Thiel, V.; Peckmann, J.; Seifert, R.; Wehrung, P.; Reitner, J.; Michaelis, W. Highly isotopically depleted isoprenoids: Molecular markers for ancient methane venting. *Geochimi. Cosmochimi. Acta* **1999**, *63*, 3959–3966. [[CrossRef](#)]
32. Reitner, J.; Peckmann, J.; Blumenberg, M.; Michaelis, W.; Reimer, A.; Thiel, V. Concretionary methane-seep carbonates and associated microbial communities in Black Sea sediments. *Palaeogeogr. Palaeoclimatol. Palaeoecol.* **2005**, *227*, 18–30. [[CrossRef](#)]
33. Marlow, J.J.; Steele, J.A.; Ziebis, W.; Thurber, A.R.; Levin, L.A.; Orphan, V.J. Carbonate-hosted methanotrophy represents an unrecognized methane sink in the deep sea. *Nat. Commun.* **2014**, *5*, 5094. [[CrossRef](#)] [[PubMed](#)]
34. Ruff, S.E.; Biddle, J.F.; Teske, A.P.; Knittel, K.; Boetius, A.; Ramette, A. Global dispersion and local diversification of the methane seep microbiome. *Proc. Natl. Acad. Sci. USA* **2015**, *112*, 4015–4020. [[CrossRef](#)] [[PubMed](#)]
35. Gieskes, J.; Mahn, C.; Day, S.; Martin, J.B.; Greinert, J.; Rathburn, T.; McAdoo, B. A study of the chemistry of pore fluids and authigenic carbonates in methane seep environments: Kodiak Trench, Hydrate Ridge, Monterey Bay, and Eel River Basin. *Chem. Geol.* **2005**, *220*, 329–345. [[CrossRef](#)]
36. Teichert, B.M.A.; Bohrmann, G.; Suess, E. Chemoherms on Hydrate Ridge — Unique microbially-mediated carbonate build-ups growing into the water column. *Palaeogeogr. Palaeoclimatol. Palaeoecol.* **2005**, *227*, 67–85. [[CrossRef](#)]
37. Birgel, D.; Himmler, T.; Freiwald, A.; Peckmann, J. A new constraint on the antiquity of anaerobic oxidation of methane: Late Pennsylvanian seep limestones from southern Namibia. *Geology* **2008**, *36*, 543–546. [[CrossRef](#)]

38. Marlow, J.J.; Steele, J.A.; Case, D.H.; Connon, S.A.; Levin, L.A.; Orphan, V.J. Microbial abundance and diversity patterns associated with sediments and carbonates from the methane seep environments of Hydrate Ridge, OR. *Front. Mar. Sci.* **2014**, *1*, 44. [[CrossRef](#)]
39. Case, D.H.; Pasulka, A.L.; Marlow, J.J.; Grupe, B.M.; Levin, L.A.; Orphan, V.J. Methane seep carbonates host distinct, diverse, and dynamic microbial assemblages. *MBio* **2015**, *6*, e01348-15. [[CrossRef](#)]
40. Matsumoto, R.; Okuda, Y.; Aoyama, C.; Hiruta, A.; Ishida, Y.; Sunamura, M.; Numanami, H.; Tomaru, H.; Snyder, G.T.; Komatsubara, J.; et al. Methane plumes over a marine gas hydrate system in the eastern margin of Japan Sea: A possible mechanism for the transportation of subsurface methane to shallow waters. In Proceedings of the Fifth International Conference on Gas Hydrate, Trondheim, Norway, 13–16 June 2005.
41. Matsumoto, R.; Kakuwa, Y.; Tanahashi, M. Occurrence and origin of shallow gas hydrates of the eastern margin of Japan Sea as revealed by Calypso and CASQ corings of R/V Marion Dufresne. In Proceedings of the 7th International Conference on Gas Hydrates, Scotland, UK, 17–21 July 2011.
42. Tomaru, H.; Lu, Z.L.; Snyder, G.T.; Fehn, U.; Hiruta, A.; Matsumoto, R. Origin and age of pore waters in an actively venting gas hydrate field near Sado Island, Japan Sea: Interpretation of halogen and I-129 distributions. *Chem. Geol.* **2007**, *236*, 350–366. [[CrossRef](#)]
43. Hachikubo, A.; Yanagawa, K.; Tomaru, H.; Lu, H.; Matsumoto, R. Molecular and isotopic composition of volatiles in gas hydrates and in sediment from the Joetsu Basin, eastern margin of the Japan Sea. *Energies* **2015**, *8*, 4647–4666. [[CrossRef](#)]
44. Freire, A.F.M.; Matsumoto, R.; Santos, L.A. Structural-stratigraphic control on the Umitaka Spur gas hydrates of Joetsu Basin in the eastern margin of Japan Sea. *Mar. Pet. Geol.* **2011**, *28*, 1967–1978. [[CrossRef](#)]
45. Kano, A.; Miyahara, R.; Yanagawa, K.; Mori, T.; Owari, S.; Tomaru, H.; Kakizaki, Y.; Snyder, G.; Shimono, T.; Kakuwa, Y.; et al. Gas hydrate estimates in muddy sediments from the oxygen isotope of water fraction. *Chem. Geol.* **2017**, *470*, 107–115. [[CrossRef](#)]
46. Kouduka, M.; Tanabe, A.S.; Yamamoto, S.; Yanagawa, K.; Nakamura, Y.; Akiba, F.; Tomaru, H.; Toju, H.; Suzuki, Y. Eukaryotic diversity in late Pleistocene marine sediments around a shallow methane hydrate deposit in the Japan Sea. *Geobiology* **2017**, *15*, 715–727. [[CrossRef](#)] [[PubMed](#)]
47. Yanagawa, K.; Kouduka, M.; Nakamura, Y.; Hachikubo, A.; Tomaru, H.; Suzuki, Y. Distinct microbial communities thriving in gas hydrate-associated sediments from the eastern Japan Sea. *J. Asian Earth Sci.* **2014**, *90*, 243–249. [[CrossRef](#)]
48. Yanagawa, K.; Sunamura, M.; Lever, M.A.; Morono, Y.; Hiruta, A.; Ishizaki, O.; Matsumoto, R.; Urabe, T.; Inagaki, F. Niche separation of methanotrophic archaea (ANME-1 and -2) in methane-seep sediments of the eastern Japan Sea offshore Joetsu. *Geomicrobiol. J.* **2011**, *28*, 118–129. [[CrossRef](#)]
49. Yanagawa, K.; Tani, A.; Yamamoto, N.; Hachikubo, A.; Kano, A.; Matsumoto, R.; Suzuki, Y. Biogeochemical Cycle of Methanol in Anoxic Deep-Sea Sediments. *Microbes Environ.* **2016**, *31*, 190–193. [[CrossRef](#)]
50. Manheim, F.T.; Brooks, E.G.; Winters, W.J. *Description of A Hydraulic Sediment Squeezer*; Citeseer: Princeton, NJ, USA, 1994; pp. 94–584.
51. Tomaru, H.; Fehn, U.; Lu, Z.; Takeuchi, R.; Inagaki, F.; Imachi, H.; Kotani, R.; Matsumoto, R.; Aoike, K. Dating of Dissolved Iodine in Pore Waters from the Gas Hydrate Occurrence Offshore Shimokita Peninsula, Japan: ¹²⁹I Results from the D/V *Chikyū* Shakedown Cruise. *Resour. Geol.* **2009**, *59*, 359–373. [[CrossRef](#)]
52. Sarazin, G.; Michard, G.; Prevot, F. A rapid and accurate spectroscopic method for alkalinity measurements in sea water samples. *Water Res.* **1999**, *33*, 290–294. [[CrossRef](#)]
53. Yanagawa, K.; Morono, Y.; Yoshida-Takashima, Y.; Eitoku, M.; Sunamura, M.; Inagaki, F.; Imachi, H.; Takai, K.; Nunoura, T. Variability of subseafloor viral abundance at the geographically and geologically distinct continental margins. *FEMS Microbiol. Ecol.* **2014**, *88*, 60–68. [[CrossRef](#)]
54. Takai, K.; Horikoshi, K. Rapid detection and quantification of members of the archaeal community by quantitative PCR using fluorogenic probes. *Appl. Environ. Microbiol.* **2000**, *66*, 5066–5072. [[CrossRef](#)]
55. Nunoura, T.; Oida, H.; Miyazaki, J.; Miyashita, A.; Imachi, H.; Takai, K. Quantification of mcrA by fluorescent PCR in methanogenic and methanotrophic microbial communities. *FEMS Microbiol. Ecol.* **2008**, *64*, 240–247. [[CrossRef](#)] [[PubMed](#)]
56. Ludwig, W.; Strunk, O.; Westram, R.; Richter, L.; Meier, H.; Yadhukumar; Buchner, A.; Lai, T.; Steppi, S.; Jobb, G.; et al. ARB: A software environment for sequence data. *Nucleic. Acids. Res.* **2004**, *32*, 1363–1371. [[CrossRef](#)] [[PubMed](#)]

57. Caporaso, J.G.; Lauber, C.L.; Walters, W.A.; Berg-Lyons, D.; Lozupone, C.A.; Turnbaugh, P.J.; Fierer, N.; Knight, R. Global patterns of 16S rRNA diversity at a depth of millions of sequences per sample. *Proc. Natl. Acad. Sci. USA* **2011**, *108*, 4516–4522. [[CrossRef](#)] [[PubMed](#)]
58. Bolyen, E.; Rideout, J.R.; Dillon, M.R.; Bokulich, N.A.; Abnet, C.C.; Al-Ghalith, G.A.; Alexander, H.; Alm, E.J.; Arumugam, M.; Asnicar, F.; et al. Reproducible, interactive, scalable and extensible microbiome data science using QIIME 2. *Nat. Biotechnol.* **2019**, *37*, 852–857. [[CrossRef](#)] [[PubMed](#)]
59. Reeburgh, W.S. Oceanic methane biogeochemistry. *Chem. Rev.* **2007**, *107*, 486–513. [[CrossRef](#)] [[PubMed](#)]
60. Borowski, W.S.; Paull, C.K.; Ussler, W. Marine pore-water sulfate profiles indicate in situ methane flux from underlying gas hydrate. *Geology* **1996**, *24*, 655–658. [[CrossRef](#)]
61. Naehr, T.H.; Eichhubl, P.; Orphan, V.J.; Hovland, M.; Paull, C.K.; Ussler, W.; Lorenson, T.D.; Greene, H.G. Authigenic carbonate formation at hydrocarbon seeps in continental margin sediments: A comparative study. *Deep Sea Res. Part II Top. Stud. Oceanogr.* **2007**, *54*, 1268–1291. [[CrossRef](#)]
62. Reitner, J.; Peckmann, J.; Reimer, A.; Schumann, G.; Thiel, V. Methane-derived carbonate build-ups and associated microbial communities at cold seeps on the lower Crimean shelf (Black Sea). *Facies* **2005**, *51*, 66–79. [[CrossRef](#)]
63. Hallam, S.J.; Girguis, P.R.; Preston, C.M.; Richardson, P.M.; DeLong, E.F. Identification of methyl coenzyme M reductase A (*mcrA*) genes associated with methane-oxidizing archaea. *Appl. Environ. Microbiol.* **2003**, *69*, 5483–5491. [[CrossRef](#)]
64. Knittel, K.; Lösekann, T.; Boetius, A.; Kort, R.; Amann, R. Diversity and distribution of methanotrophic archaea at cold seeps. *Appl. Environ. Microbiol.* **2005**, *71*, 467–479. [[CrossRef](#)]
65. Torres, M.E.; Wallmann, K.; Tréhu, A.M.; Bohrmann, G.; Borowski, W.S.; Tomaru, H. Gas hydrate growth, methane transport, and chloride enrichment at the southern summit of Hydrate Ridge, Cascadia margin off Oregon. *Earth. Planet. Sci. Lett.* **2004**, *226*, 225–241. [[CrossRef](#)]
66. Blumenberg, M.; Walliser, E.-O.; Taviani, M.; Seifert, R.; Reitner, J. Authigenic carbonate formation and its impact on the biomarker inventory at hydrocarbon seeps—A case study from the Holocene Black Sea and the Plio-Pleistocene Northern Apennines (Italy). *Mar. Pet. Geol.* **2015**, *66*, 532–541. [[CrossRef](#)]
67. Boivin-Jahns, V.; Ruimy, R.; Bianchi, A.; Daumas, S.; Christen, R. Bacterial diversity in a deep-subsurface clay environment. *Appl. Environ. Microbiol.* **1996**, *62*, 3405–3412. [[PubMed](#)]
68. Zhou, J.; Xia, B.; Huang, H.; Palumbo, A.V.; Tiedje, J.M. Microbial diversity and heterogeneity in sandy subsurface soils. *Appl. Environ. Microbiol.* **2004**, *70*, 1723–1734. [[CrossRef](#)] [[PubMed](#)]
69. Niemann, H.; Lösekann, T.; de Beer, D.; Elvert, M.; Nadalig, T.; Knittel, K.; Amann, R.; Sauter, E.J.; Schluter, M.; Klages, M.; et al. Novel microbial communities of the Haakon Mosby mud volcano and their role as a methane sink. *Nature* **2006**, *443*, 854–858. [[CrossRef](#)] [[PubMed](#)]
70. Felden, J.; Ruff, S.E.; Ertefai, T.; Inagaki, F.; Hinrichs, K.-U.; Wenzhöfer, F. Anaerobic methanotrophic community of a 5346-m-deep vesicomyid clam colony in the Japan Trench. *Geobiology* **2014**, *12*, 183–199. [[CrossRef](#)] [[PubMed](#)]
71. Pop Ristova, P.; Wenzhöfer, F.; Ramette, A.; Felden, J.; Boetius, A. Spatial scales of bacterial community diversity at cold seeps (Eastern Mediterranean Sea). *ISME J.* **2015**, *9*, 1306–1318. [[CrossRef](#)] [[PubMed](#)]
72. Fry, J.C.; Parkes, R.J.; Cragg, B.A.; Weightman, A.J.; Webster, G. Prokaryotic biodiversity and activity in the deep subseafloor biosphere. *FEMS Microbiol. Ecol.* **2008**, *66*, 181–196. [[CrossRef](#)] [[PubMed](#)]
73. Girguis, P.R.; Cozen, A.E.; DeLong, E.F. Growth and population dynamics of anaerobic methane-oxidizing archaea and sulfate-reducing bacteria in a continuous-flow bioreactor. *Appl. Environ. Microbiol.* **2005**, *71*, 3725–3733. [[CrossRef](#)]
74. Timmers, P.; Widjaja-Greefkes, H.C.; Ramiro-Garcia, J.; Plugge, C.; Stams, A. Growth and activity of ANME clades with different sulfate and sulfide concentrations in the presence of methane. *Front. Microbiol.* **2015**, *6*, 998. [[CrossRef](#)]
75. Harrison, B.K.; Zhang, H.; Berelson, W.; Orphan, V.J. Variations in archaeal and bacterial diversity associated with the sulfate-methane transition zone in continental margin sediments (Santa Barbara Basin, California). *Appl. Environ. Microbiol.* **2009**, *75*, 1487–1499. [[CrossRef](#)] [[PubMed](#)]
76. Krüger, M.; Blumenberg, M.; Kasten, S.; Wieland, A.; Kanel, L.; Klock, J.H.; Michaelis, W.; Seifert, R. A novel, multi-layered methanotrophic microbial mat system growing on the sediment of the Black Sea. *Environ. Microbiol.* **2008**, *10*, 1934–1947. [[CrossRef](#)] [[PubMed](#)]

77. Niu, M.; Fan, X.; Zhuang, G.; Liang, Q.; Wang, F. Methane-metabolizing microbial communities in sediments of the Haima cold seep area, northwest slope of the South China Sea. *FEMS Microbiol. Ecol.* **2017**, *93*, fix101. [[CrossRef](#)] [[PubMed](#)]
78. Nunoura, T.; Oida, H.; Toki, T.; Ashi, J.; Takai, K.; Horikoshi, K. Quantification of *mcrA* by quantitative fluorescent PCR in sediments from methane seep of the Nankai Trough. *FEMS Microbiol. Ecol.* **2006**, *57*, 149–157. [[CrossRef](#)] [[PubMed](#)]
79. Orcutt, B.; Boetius, A.; Elvert, M.; Samarkin, V.; Joye, S.B. Molecular biogeochemistry of sulfate reduction, methanogenesis and the anaerobic oxidation of methane at Gulf of Mexico cold seeps. *Geochim. Cosmochim. Acta* **2005**, *69*, 4267–4281. [[CrossRef](#)]
80. Hinrichs, K.U.; Boetius, A. The anaerobic oxidation of methane: new insights in microbial ecology and biogeochemistry. In *Ocean Margin Systems*; Wefer, G., Billett, D., Hebbeln, D., Jørgensen, B.B., Schlüter, M., Weering, T.V., Eds.; Springer: Berlin, Germany, 2002; pp. 457–477.
81. Boetius, A.; Wenzhöfer, F. Seafloor oxygen consumption fuelled by methane from cold seeps. *Nat. Geosci.* **2013**, *6*, 725. [[CrossRef](#)]
82. Klauke, I.; Masson, D.G.; Petersen, C.J.; Weinrebe, W.; Ranero, C.R. Multifrequency geoacoustic imaging of fluid escape structures offshore Costa Rica: Implications for the quantification of seep processes. *Geochem. Geophys. Geosyst.* **2008**, *9*. [[CrossRef](#)]



© 2019 by the authors. Licensee MDPI, Basel, Switzerland. This article is an open access article distributed under the terms and conditions of the Creative Commons Attribution (CC BY) license (<http://creativecommons.org/licenses/by/4.0/>).